

Functional Inference on Rotational Curves and Identification of Human Gait at the Knee Joint

Fabian J.E. Telschow*, Stephan F. Huckemann* and Michael R. Pierrynowski†

Abstract

We extend Gaussian perturbation models in classical functional data analysis to the three-dimensional rotational group where a zero-mean Gaussian process in the Lie algebra under the Lie exponential spreads multiplicatively around a central curve. As an estimator, we introduce point-wise extrinsic mean curves which feature strong perturbation consistency, and which are asymptotically a.s. unique and differentiable, if the model is so. Further, we consider the group action of time warping and that of spatial isometries that are connected to the identity. The latter can be asymptotically consistently estimated if lifted to the unit quaternions. Introducing a generic loss for Lie groups, the former can be estimated, and based on curve length, due to asymptotic differentiability, we propose two-sample permutation tests involving various combinations of the group actions. This methodology allows inference on gait patterns due to the rotational motion of the lower leg with respect to the upper leg. This was previously not possible because, among others, the usual analysis of separate Euler angles is not independent of marker placement, even if performed by trained specialists.

1 Introduction

To date a rich set of powerful descriptive and inferential tools are available for the statistical goals of *functional data analysis* (FDA) as coined by Ramsay (1982). For a recent overview, see Wang et al. (2015). Beyond classical Euclidean FDA, currently, functional data taking values in manifolds is gaining increased interest. For instance the work of Srivastava et al. (2011) has spurred several subsequent publications, e.g. Celledoni and Eslitzbichler (2015); Bauer et al. (2015, 2016); Amor et al. (2016). At this point, however, inferential tools, for manifold valued curves, say, are not yet available, although, as an important step, a general time warping method has been developed by Su et al. (2014).

In this paper we propose a nonparametric two-sample test for functional data that takes values in the rotational group $SO(3)$. Like a classical two sample test it relies on the concept of a mean, in our case, a mean curve. With this endeavor, there are three challenges.

First, unlike Euclidean spaces, in any of the non-Euclidean geometries of $SO(3)$ there is no a priori guarantee that the mean is unique and that its estimators feature favorable statistical properties. Second, it is not clear which from the “zoo” of generalizations (e.g. Huckemann (2012)) of the classical Euclidean mean to a curved space should be taken. Third, temporal and spatial registration require specific non-Euclidean loss functions, that should at least be invariant under reparametrization (temporal) and actions of isometries (spatial).

To these ends, naturally generalizing the common functional model in \mathbb{R}^D

$$y(t) = \mu(t) + Z_t, \quad (1)$$

where μ is deterministic and Z_t is a zero-mean multivariate Gaussian process, we develop the framework of *Gaussian perturbation* (GP) models

$$y(t) = \mu(t)\text{Exp}(Z_t), \quad (2)$$

*Felix Bernstein Institute for Mathematical Statistics in the Biosciences, Georgia Augusta University of Göttingen, Goldschmidtstrasse 7, 37077 Göttingen, Germany

†School of Rehabilitation Science, McMaster University, Canada

in which a zero-mean Gaussian process Z_t in the Lie algebra under the Lie exponential Exp spreads multiplicatively around a central curve μ . This is indeed a generalization because \mathbb{R}^D can be viewed as an additive Lie group agreeing with its Lie algebra, such that the Lie exponential is the identity and the “multiplication” in (2) is then just the summation in (1). In fact, we will see that our GP models are canonical in that way that the class of models due to multiplication from the right as in (2) is equal to class of models due to multiplication from the left and asymptotically, as the noise level vanishes, equal to models due to multiplication from both sides. In non-functional settings analog models were studied and used in Downs (1972), Rancourt et al. (2000) and Fletcher (2011).

Defining the *pointwise extrinsic Fréchet mean* (PEM) curve we show strong asymptotic consistency, namely that PEM curves converge a.s. to the central curve. This is rather unusual as *perturbation consistency* is often not given, even if the noise is isotropic, e.g. Kent and Mardia (1997); Huckemann (2011). Here it holds under very general conditions, in particular for our GP models which do not require isotropicity. Moreover, in view of our tests based on curve lengths, thus requiring existence of derivatives or at least absolute continuity, we show that for a.s. \mathcal{C}^1 (continuously differentiable) GP models, asymptotically sample PEM curves are again \mathcal{C}^1 .

Further we model spatial registration by the action of the identity component of the isometry group on $SO(3)$. In a Euclidean geometry, these correspond to orientation preserving Euclidean motions. While for this action, a new loss induced from lifting to the unit quaternions, allows for asymptotically strongly consistent registration, for temporal alignment we define another new loss function which is canonical on any Lie group. Thus we can avoid the generic method for temporal alignment on manifolds proposed by Su et al. (2014) which suffers from non-canonical choices such as parallel transport to a reference tangent space. These facts combined with the equivariance of GP models under both group actions are used to formulate nonparametric two-sample permutation tests with and without spatial and/or temporal registration based on lengths of sample PEM curves.

Notably, some of our ideas generalize to $SO(n)$ (for instance, for odd dimension n , the group is still simple and hence the identity component of the group of spatial isometries is again given by $SO(n) \times SO(n)$, cf. Lemma 2.1) and GP models (2) in conjunction with the loss functions and their temporal invariance and inverse alignment properties can, of course, be defined on any Lie group. For a concise presentation, we have restricted ourselves to $SO(3)$ which allows fast spatial registration using the double cover of rotations by unit quaternions.

This research has been motivated by the long standing problem of reproducibility of gait curves in the biomechanical analysis of motion (see Duhamel et al. (2004)). Here, studying trajectories of the relative rotations between tibia (the lower leg’s main bone) with respect to the femur (the upper leg’s bone) originating from typical walking motion is of interest, for instance in order to assess various degenerative processes (e.g., early onset of osteoarthritis, see Pierrynowski et al. (2010)), as well as to evaluate therapeutic interventions (see Öunpuu et al. (2015)).

Unless invasive methods such as fluoroscopic (X-ray) imaging are used, in common practice the underlying bone motion must be estimated. Markers are placed on specific skin locations of subjects, and the 3D motion of these markers are recorded while subjects perform certain walking tasks. It is well known, however, that such methods introduce *soft tissue artifacts* (e.g., Leardini et al. (2005)) because they also include skin, muscle and fat tissue motion which are superimposed over the unknown bone’s motion.

We identify here another effect that influences the measurement of the underlying bone motion. Specialists place markers on anatomically defined skin locations and a calibration of relative coordinate frames is performed. However, the ability of specialists to place these markers repeatedly is questionable (see Noehren et al. (2010) and Groen et al. (2012)). In an experiment performed we see a notable deviation between the three Euler angle curves of relative rotations, as defined in Grood and Suntay (1983), before and after specialist marker replacement, see Figure 1a. Since the bottom internal-external rotation angles are considerably vertically shifted, a test based on all three Euler angles would reject the identity of the same subject with itself after trained specialist replacement. It seems that this effect has hampered the development of testing protocols that can reliably identify subjects when nothing changed but specialist *marker placements* (MP). However, such identifications are a sine qua non for detecting changes in gait patterns due to degenerative

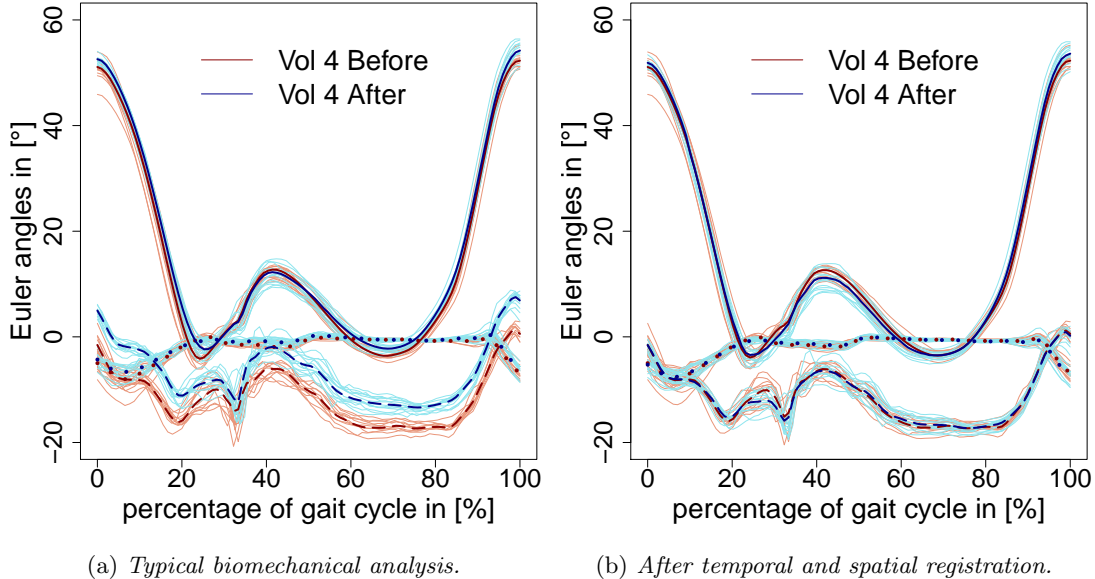


Figure 1: *Depicting two samples of three Euler angle curves (top: flexion-extension, middle: abduction-adduction and bottom: internal-external rotation) determining motion at the knee joint for the same subject (volunteer 4) before (red) and after specialist marker replacement (blue). Bold face curves represent sample PEM curves. Left (a): raw data as processed using typical biomechanical analysis. Note the vertical shift of the bottom internal-external rotation angles. Right (b): After temporal and spatial registration, the vertical shift has been removed along with other smaller distortions.*

effects or evaluate the effects of therapy. We will see that our permutation tests including spatial-temporal registration robustly remove this MP effect, see Figure 1b, and allow for the development of inferential protocols in the future. These could then be applied to biomechanical analysis at other body joints as well.

Our paper is organized as follows. In Section 2, after some background information on geometry, we introduce the data space with the two group actions and define \mathcal{C}^1 GP models with a discussion on their canonicity. We then introduce Fréchet mean estimators and derive their benign properties in GP models. Section 3 deals with the estimation of spatial and temporal registration. Having provided for all of the ingredients, we propose our two-sample tests in Section 4, provide for simulations in Section 5 and apply in Section 6 our new methodology to a biomechanical experiment conducted in the School of Rehabilitation Science at McMaster University (Canada).

Unless otherwise stated, all of the proofs have been deferred to the Appendix.

2 Functional Data Model For Rotational Curves

2.1 The Rotational Group and Its Isometries

In the following G denotes the compact connected Lie group of three-dimensional rotations $G = SO(3)$ which comes with the Lie algebra $\mathfrak{g} = \mathfrak{so}(3) = \{A \in \mathbb{R}^{3 \times 3} : A^T = -A\}$ of 3×3 skew symmetric matrices. This Lie algebra is a three-dimensional linear subspace of all 3×3 matrices and thus carries the natural structure of \mathbb{R}^3 conveyed by the isomorphism $\iota : \mathbb{R}^3 \rightarrow \mathfrak{so}(3)$ given by

$$\iota(a) = \begin{pmatrix} 0 & -a_3 & a_2 \\ a_3 & 0 & -a_1 \\ -a_2 & a_1 & 0 \end{pmatrix}, \quad \text{for } a = (a_1, a_2, a_3)^T \in \mathbb{R}^3.$$

This isomorphism exhibits at once the following relation

$$Q\iota(a)Q^T = \iota(Qa) \text{ for all } a \in \mathbb{R}^3 \text{ and } Q \in G. \quad (3)$$

We use the scalar product $\langle A, B \rangle = \text{trace}(AB^T)/2$, which induces the rescaled Frobenius norm $\|A\| = \sqrt{\text{trace}(AA^T)/2}$, on all matrix spaces considered in this paper. On all subspaces it induces the *extrinsic metric*, cf. Bhattacharya and Patrangenaru (2003). Moreover, we denote with $I_{3 \times 3}$ the unit matrix. As usual, $A \mapsto \text{Exp}(A)$ denotes the matrix exponential which is identical to the Lie exponential and gives a surjection $\mathfrak{g} \rightarrow G$. Due to skew symmetry, the following *Rodriguez formula* holds

$$\text{Exp}(A) = \sum_{j=0}^{\infty} \frac{A^j}{j!} = I_{3 \times 3} + \frac{\sin(\|A\|)}{\|A\|} A + \frac{1 - \cos(\|A\|)}{\|A\|^2} A^2. \quad (4)$$

This yields that the Lie exponential is bijective on $\mathcal{B}_\pi(0) = \{A \in \mathfrak{g} : \|A\| < \pi\}$. For a detailed discussion, see (Chirikjian and Kyatkin 2000, p. 121).

The scalar product on the Lie algebra is invariant under left and right multiplication from G i.e., $\langle A, B \rangle = \langle PAQ, PBQ \rangle$ for all $P, Q \in G$ and it induces a bi-invariant Riemannian metric on all tangent spaces $\mathcal{T}_P G$ ($P \in G$) via

$$\langle v, w \rangle_P = \left\langle (dL_P)^{-1}v, (dL_P)^{-1}w \right\rangle,$$

where $v, w \in \mathcal{T}_P G$, $P \in G$ and $L_P : G \rightarrow G, Q \mapsto L(Q) = PQ$ is *left multiplication* by P .

The induced metric $d_{SO(3)}$ on $SO(3)$ can be simply computed from the extrinsic metric

$$d_{SO(3)}(P, Q) = 2 \arcsin \frac{\|P - Q\|}{2}, \quad (5)$$

e.g. Stanfill et al. (2013, Section 2.2), who have an additional factor $1/\sqrt{2}$ in the fraction that is absorbed in our definition of the norm.

The space of isometries with respect to this metric will be denoted with $\mathcal{I}(G)$ and its connected component containing the identity map with $\mathcal{I}_0(G)$. It is well known that both of these groups are Lie groups (see Myers and Steenrod (1939)).

Lemma 2.1. $\mathcal{I}_0(G) = G \times G$ which acts via $(P, Q) : G \rightarrow G, R \mapsto PRQ$.

2.2 Data Space and Group Actions

Recalling that $G = SO(3)$ we introduce the *data space*

$$\mathcal{X} = \mathcal{C}^1([0, 1], G).$$

On \mathcal{X} we have the action of isometries $\mathcal{I}_0(G) = G \times G$ in the connectivity component of the identity – the analog of orientation preserving Euclidean motions in a Euclidean geometry – given by

$$(t \mapsto \gamma(t)) \xrightarrow{(P, Q)} (t \mapsto P\gamma(t)Q)$$

for all $(P, Q) \in G \times G$ and $\gamma \in \mathcal{X}$, as well as the action of the group (by composition) of time reparametrizations

$$\text{Diff}^+[0, 1] = \left\{ \phi \in \mathcal{C}^\infty([0, 1], [0, 1]) \mid \phi'(t) > 0 \text{ for all } t \in (0, 1) \right\}$$

given by

$$(t \mapsto \gamma(t)) \xrightarrow{\phi} (t \mapsto \gamma \circ \phi(t)).$$

for all $\phi \in \text{Diff}^+[0, 1]$ and $\gamma \in \mathcal{X}$. Of course, both group actions commute and we can define the direct product group

$$\mathcal{I}_0(G) \times \text{Diff}^+[0, 1].$$

In the following, when we speak of the *similarity group* \mathcal{S} acting, we either refer to the spatial action by $\mathcal{S} = \mathcal{I}_0(G)$, or the temporal action by $\mathcal{S} = \text{Diff}^+[0, 1]$, or the joint action by $\mathcal{S} = \mathcal{I}_0(G) \times \text{Diff}^+[0, 1]$. Any of the three group actions will be denoted by $G \xrightarrow{g} G$, $P \mapsto g.P$ for every $g \in \mathcal{S}$.

2.3 Gaussian Perturbation Models

Definition 2.2. *We say that a random curve $\gamma \in \mathcal{X}$ follows a Gaussian perturbation (GP) around a center curve $\gamma_0 \in \mathcal{X}$, if there is a \mathbb{R}^3 -valued zero-mean Gaussian processes A_t with a.s. \mathcal{C}^1 paths, such that*

$$\gamma(t) = \gamma_0(t)\text{Exp}(\iota \circ A_t), \quad (6)$$

for all $t \in [0, 1]$. The Gaussian process A_t will be called the generating process.

From the fact that,

$$Q\text{Exp}(A)Q^T = \text{Exp}(QAQ^T) \text{ for all } Q \in G \text{ and } A \in \mathfrak{g} \quad (7)$$

we obtain at once the following Theorem.

Theorem 2.3 (Invariance of GP Models under Spatial and Temporal Group Actions). *Let $(P, Q) \in \mathcal{I}_0(G)$, $\phi \in \text{Diff}^+[0, 1]$ and let $\gamma \in \mathcal{X}$ follow a GP around a center curve $\gamma_0 \in \mathcal{X}$. Then $P(\gamma \circ \phi)Q$ follows a GP around the center curve $P(\gamma_0 \circ \phi)Q$.*

Since G is non-commutative, GP models as introduced above are not the only canonical generalization of the models (1). Instead of the perturbation model (6), which is a detailed version of (2), involving an a.s. \mathcal{C}^1 -Gaussian process from the right, one could also consider perturbation models involving an a.s. \mathcal{C}^1 -Gaussian process B_t from the left, or even from both sides, involving a.s. \mathcal{C}^1 -Gaussian processes C_t and D_t i.e.,

$$\eta(t) = \text{Exp}(\iota \circ B_t) \eta_0(t) \quad (8)$$

$$\delta(t) = \text{Exp}(\iota \circ C_t) \delta_0(t) \text{Exp}(\iota \circ D_t) \quad (9)$$

for all $t \in [0, 1]$. Again, invoking (7) the following Theorem follows readily.

Theorem 2.4. *Any GP model (6) can be rewritten into a left Gaussian perturbation model (8) with the same center curve $\gamma_0 \in \mathcal{X}$ i.e., for any a.s. \mathcal{C}^1 Gaussian process A_t there exists an a.s. \mathcal{C}^1 Gaussian process B_t such that*

$$\gamma_0(t)\text{Exp}(\iota \circ A_t) = \text{Exp}(\iota \circ B_t)\gamma_0(t)$$

and vice versa.

Theorem 2.5. *Let $\sigma \rightarrow 0$ be a concentration parameter. Consider a both-sided Gaussian perturbation $\delta(t)$ around a center curve $\delta_0(t)$ given by (9) with $\max_{t \in [0, 1]} \|C_t\| = \mathcal{O}_p(\sigma)$ and $\max_{t \in [0, 1]} \|D_t\| = \mathcal{O}_p(\sigma)$ for all $t \in [0, 1]$. Then $\delta(t)$ can be rewritten into a right Gaussian perturbation i.e.,*

$$\delta(t) = \delta_0(t) \text{Exp}(\iota \circ A_t + \iota \circ \tilde{A}_t)$$

with an a.s. \mathcal{C}^1 zero-mean Gaussian process $A_t = \delta_0(t)^T C_t + D_t$ and a suitable zero-mean a.s. \mathcal{C}^1 process \tilde{A}_t satisfying $\max_{t \in [0, 1]} \|\tilde{A}_t\| = \mathcal{O}_p(\sigma^2)$.

Remark 2.6. *Of course, every right Gaussian perturbation (6) or left Gaussian perturbation (6) is also a both sided Gaussian perturbation (9), since the deterministic process $C_t = 0$ or $D_t = 0$ for all $t \in [0, 1]$ is a Gaussian process by definition.*

2.4 Asymptotic Properties of Center Curve Estimates

For the entire paper we consider the canonical embedding $G = SO(3) \hookrightarrow \mathbb{R}^{3 \times 3}$. For random curves $\gamma_1, \dots, \gamma_N, \gamma \in \mathcal{X}$ denote with

$$\bar{\gamma}_N(t) = N^{-1} \sum_{n=1}^N \gamma_n(t) \in \mathbb{R}^{3 \times 3},$$

the usual Euclidean average curve and by $\mathbb{E}[\gamma(t)] \in \mathbb{R}^{3 \times 3}$ the usual expected curve, if existent.

Definition 2.7. For random curves $\gamma_1, \dots, \gamma_N, \gamma \in \mathcal{X}$, every curve $\mu : [0, 1] \rightarrow G$ is called a pointwise extrinsic Fréchet mean (PEM) curve, if

$$\mu(t) \in \operatorname{argmin}_{\mu \in G} \mathbb{E}[\|\mu - \gamma(t)\|^2], \quad \text{this is a population PEM curve, or}$$

$$\mu(t) \in \hat{E}_N(t) = \operatorname{argmin}_{\mu \in G} \frac{1}{N} \sum_{n=1}^N \|\mu - \gamma_n(t)\|^2, \quad \text{this is a sample PEM curve,}$$

respectively.

Due to compactness of G there are always PEM curves. Verify at once the following equivariance property.

Theorem 2.8. Every population or sample PEM curve is an equivariant descriptor under the action of $\mathcal{I}_0(G)$ and $\operatorname{Diff}^+[0, 1]$ i.e. if $t \mapsto \mu(t)$ is a population PEM curve for $\gamma \in \mathcal{X}$ or a sample PEM curve for $\gamma_1, \dots, \gamma_N \in \mathcal{X}$ and $(P, Q) \in \mathcal{I}_0(G)$, $\phi \in \operatorname{Diff}^+[0, 1]$, then so is

$$t \mapsto P(\mu \circ \phi)(t)Q$$

a population PEM curve for $P(\gamma \circ \phi)Q$, or a sample PEM curve for $P(\gamma_1 \circ \phi)Q, \dots, P(\gamma_N \circ \phi)Q$, respectively.

In the following we are concerned with circumstances under which PEM curves are unique, again members of \mathcal{X} , and consistent estimators of a GP model's center curve. To this end recall the orthogonal projection

$$\operatorname{pr} : \mathbb{R}^{3 \times 3} \rightarrow SO(3), \quad A \mapsto \operatorname{argmin}_{\mu \in G} \|A - \mu\|^2 = \operatorname{argmax}_{\mu \in G} \operatorname{trace}(A^T \mu)$$

which is well defined if and only if $\operatorname{rank}(A) > 1$. In this case it assumes the value

$$\operatorname{pr}(A) = USV^T$$

where $A = UDV^T$ is a singular value decomposition (SVD) with decreasing eigenvalues $d_1 \geq d_2 \geq d_3 \geq 0$, $D = \operatorname{diag}(d_1, d_2, d_3)$, and

$$S = \begin{cases} I_{3 \times 3} & \text{if } \det(UV) = 1 \\ \operatorname{diag}(1, 1, -1) & \text{if } \det(UV) = -1 \end{cases},$$

e.g. Umeyama (1991, Lemma, p. 377).

Theorem 2.9. Let $\gamma_1, \dots, \gamma_N$ be a sample of a random curve $\gamma \in \mathcal{X}$. Then the following hold.

- (i) Their population or sample PEM curve is unique if and only if $\operatorname{rank}(\mathbb{E}[\gamma(t)]) > 1$, or $\operatorname{rank}(\bar{\gamma}_N(t)) > 1$, respectively, for all $t \in [0, 1]$, and it is then given by

$$t \mapsto \operatorname{pr}(\mathbb{E}[\gamma(t)]), \quad \text{or } t \mapsto \operatorname{pr}(\bar{\gamma}_N(t)),$$

respectively;

(ii) in that case the sample PEM is in \mathcal{X} and the population PEM is in \mathcal{X} if additionally $\|\dot{\gamma}(t)\| \leq Z_t$ with a process Z_t that is integrable for all $t \in [0, 1]$.

Theorem 2.10 (Perturbation Consistency). *If a random curve $\gamma \in \mathcal{X}$ follows a GP around a center curve $\gamma_0 \in \mathcal{X}$, then its PEM is curve unique and it is identical to γ_0 .*

Remark 2.11. *Close inspection of the proof of the above theorem shows that perturbation consistency is valid far beyond GP models. More precisely, for every perturbation model $\gamma(t) = \gamma_0(t)\text{Exp}(\iota \circ A_t)$ on G around any central curve γ_0 , induced by any \mathbb{R}^3 -valued stochastic process A_t satisfying*

$$\mathbb{E}[A_t \text{sinc}\|A_t\|] = 0 \quad \text{and} \quad \mathbb{E}[\cos\|A_t\|] > 0,$$

its PEM curve is unique and equal to γ_0 . Moreover, $\det(\mathbb{E}[\gamma(t)]) > 0$.

Corollary 2.12. *Let $\gamma_1, \dots, \gamma_N$ be a sample of a random curve $\gamma \in \mathcal{X}$ following a GP model around a center curve γ_0 . Fixing $t \in [0, 1]$ and choosing a measurable selection $\hat{\mu}_N(t)$ of the sample PEM curves at t , then $\hat{\mu}_N(t) \rightarrow \gamma_0(t)$ almost surely.*

This, showing that the center curve can be pointwise consistently estimated, can be improved under a mild additional assumption to hold uniformly.

Theorem 2.13. *Let $\gamma_1, \dots, \gamma_N$ be a sample of a random curve $\gamma \in \mathcal{X}$ following a GP model around a center curve γ_0 and let $t \mapsto \hat{\mu}_N(t)$ be a measurable selection of $\hat{E}_N(t)$ for each time point $t \in [0, 1]$. If the generating Gaussian process A_t satisfies*

$$\mathbb{E} \left[\max_{t \in [0, 1]} \|\partial_t A_t\| \right] < \infty, \quad (10)$$

then the following hold.

- (i) *There is $\Omega' \subset \Omega$ measurable with $\mathbb{P}(\Omega') = 1$ such that for every $\omega \in \Omega'$ there is $N_\omega \in \mathbb{N}$ such that for all $N \geq N_\omega$, every $\hat{E}_N(t)$ has a unique element $\mu_N(t)$, for all $t \in [0, 1]$, and $\hat{\mu}_N \in \mathcal{X}$;*
- (ii) *$\max_{t \in [0, 1]} \|\hat{\mu}_N(t) - \gamma_0(t)\| \rightarrow 0$ and $\max_{t \in [0, 1]} d_G(\hat{\mu}_N(t), \gamma_0(t)) \rightarrow 0$ for $N \rightarrow \infty$ almost surely.*

Corollary 2.14. *With the notations and assumptions of Theorem 2.13 we have*

$$\lim_{N \rightarrow \infty} \mathbb{P}\{t \mapsto \hat{\mu}_N(t) \in \mathcal{X}\} = 1.$$

3 Curve Registration

With various applications in mind, for instance only performing spatial registration when time warping is considered as part of the signal, or temporal registration between samples but not within, when within sample time warping is relevant for the signal, in this section we consider both registration issues separately, with the option of arbitrary combinations.

We begin with a generic loss function for general Lie groups that is invariant under both group actions, which we will use for temporal registration. As we aim at keeping our methodology open for various combinations of group actions we do not aim at giving the corresponding quotient a Riemannian structure, as in Su et al. (2014), say. Rather we then also introduce a loss function specifically tailored to the fact that the unit quaternions represent a double cover of $SO(3)$ allowing to easily perform spatial registration.

3.1 Generic Loss Functions

For curves $\gamma, \eta : [0, 1] \rightarrow \mathbb{R}^D$ it is customary to consider the *total variation* (TV) loss

$$(\gamma, \eta) \mapsto \int_0^1 \|\dot{\gamma}(t) - \dot{\eta}(t)\| dt$$

if existent, which is invariant under temporal reparametrizations and spatial isometries. If \mathbb{R}^D is viewed as an additive Lie group, this loss has the following three canonical generalizations.

Definition 3.1. The intrinsic length losses on \mathcal{X} are given by

$$\delta_{I,1}(\gamma, \eta) = \text{length}(\gamma\eta^{-1}) \quad \text{and} \quad \delta_{I,2}(\gamma, \eta) = \text{length}(\gamma^{-1}\eta),$$

for $\gamma, \eta \in \mathcal{X}$. Here the length is taken with respect to the bi-invariant metric on G ,

$$\text{length}(\gamma) = \int_0^1 \|\dot{\gamma}(t)\| dt$$

and, in order to have a loss without choosing where to put the inverse, define

$$\delta_I(\gamma, \eta) = \frac{1}{2}(\delta_{I,1}(\gamma, \eta) + \delta_{I,2}(\gamma, \eta)).$$

Each of these is again invariant under temporal and spatial reparametrizing, and more.

Theorem 3.2. Let us denote with δ either $\delta_{I,1}$, $\delta_{I,2}$ or δ_I . Then the following hold

- (i) δ is symmetric.
- (ii) δ is invariant under the action of $\mathcal{S} = \mathcal{I}_0(G) \times \text{Diff}^+[0, 1]$, i.e.

$$\delta((\psi, \phi).\gamma, (\psi, \phi).\eta) = \delta(\gamma, \eta)$$

for all $(\psi, \phi) \in \mathcal{S}$ and all $\gamma, \eta \in \mathcal{X}$.

- (iii) Let $P \in G$ be arbitrary. Then $\delta_{I,1}(P\gamma, \eta) = \delta_{I,1}(\gamma, \eta)$ and $\delta_{I,2}(\gamma P, \eta) = \delta_{I,2}(\gamma, \eta)$ for all $\gamma, \eta \in \mathcal{X}$.
- (iv) $\delta_{I,1}(\gamma, \eta) = 0$ if and only if $\eta = \gamma P$ for some $P \in G$. Similarly, $\delta_{I,2}(\gamma, \eta) = 0$ if and only if $\eta = P\gamma$ for some $P \in G$.
- (v) Let $\gamma, \eta \in \mathcal{X}$. Then we have the inverse alignment property

$$(\phi^*, \psi^*) \in \underset{(\phi, \psi) \in \mathcal{S}}{\text{arginf}} \delta(\gamma_1, (\phi, \psi).\gamma_2) \Rightarrow ((\phi^*)^{-1}, (\psi^*)^{-1}) \in \underset{(\phi, \psi) \in \mathcal{S}}{\text{arginf}} \delta(\gamma_2, (\phi, \psi).\gamma_1)$$

Although all three of our intrinsic loss functions fulfill the inverse alignment property, if the infimum is attained, the joint minimization is challenging and we use minimization w.r.t. δ (i.e. $\delta_{I,1}$, $\delta_{I,2}$ or δ_I) only to obtain

$$\phi^* \in \underset{\phi \in \text{Diff}^+[0,1]}{\text{arginf}} \delta(\gamma_1, \gamma_2 \circ \phi), \tag{11}$$

using a dynamic program, following Kurtek et al. (2011); Srivastava, Wu, Kurtek, Klassen, and Marron (Srivastava et al.); Srivastava et al. (2011).

3.2 Spatial Alignment

A unit quaternion point of view allows for a direct and noniterative spatial alignment given by

$$E_{\gamma, \eta} = \underset{P, Q \in SO(3)}{\text{argmin}} L(P\gamma Q, \eta), \tag{12}$$

for $\gamma, \eta \in X$ with a loss function L induced by a suitable loss function on the unit quaternions below in (13) and (15).

The unit quaternions are given by $\mathbb{S}^3 = \{x \in \mathbb{R}^4 : \|x\| = 1\}$ equipped with a multiplicative group structure via

$$\mathbb{S}^3 \ni (x_1, x_2, x_3, x_4)^T \leftrightarrow x_1 + ix_2 + jx_3 + kx_4$$

with $i^2 = j^2 = k^2 = -1$ and $i \cdot j = -j \cdot i = k$, $k \cdot i = -i \cdot k = j$, $j \cdot k = -k \cdot j = i$ (e.g., Chirikjian and Kyatkin (2000)). Moreover, the map

$$\pi : \mathbb{S}^3 \rightarrow G$$

$$\begin{pmatrix} x_1 \\ x_2 \\ x_3 \\ x_4 \end{pmatrix} \mapsto \begin{pmatrix} 1 - 2x_3^2 - 2x_4^2 & 2(x_2x_3 + x_1x_4) & 2(x_2x_4 - x_1x_3) \\ 2(x_2x_3 - x_1x_4) & 1 - 2x_2^2 - 2x_4^2 & 2(x_3x_4 + x_1x_2) \\ 2(x_2x_4 + x_1x_3) & 2(x_3x_4 - x_1x_2) & 1 - 2x_2^2 - 2x_3^2 \end{pmatrix}$$

is a double (even universal) cover of G and a smooth surjective group homomorphism with the property $\pi(x) = \pi(-x)$ for all $x \in \mathbb{S}^3$ (see Stuepnagel (1964)). Thus, by the lifting property of covering maps (e.g., Lee (2013, Proposition A.77, p.616)) any curve $\gamma \in \mathcal{X}$ has exactly two continuous lifts $\tilde{\gamma}$ in \mathbb{S}^3 , each uniquely determined by the choice of the starting element from $\pi^{-1}(\gamma(0))$.

In consequence, every continuous loss function $\tilde{L} : \mathcal{C}([0, 1], \mathbb{S}^3) \times \mathcal{C}([0, 1], \mathbb{S}^3) \rightarrow \mathbb{R}_{\geq 0}$ invariant under common sign changes induces a continuous loss function $L : \mathcal{X} \times \mathcal{X} \rightarrow \mathbb{R}_{\geq 0}$ via

$$L(\gamma, \eta) = \min \left\{ \tilde{L}(\tilde{\gamma}, \tilde{\eta}), \tilde{L}(-\tilde{\gamma}, \tilde{\eta}) \right\} \quad (13)$$

where $\tilde{\gamma}$ and $\tilde{\eta}$ are arbitrary continuous lifts of γ and η .

The following setup now allows to compare minimizers of (12) with suitably defined minimizers for \tilde{L} because the action of $\mathcal{I}_0(G)$ on \mathcal{X} lifts to the canonical left action of $SO(4)$ on continuously lifted curves $\tilde{\gamma} \in \mathcal{C}([0, 1], \mathbb{S}^3)$ as in (14) below. The following is well known, where (i) and (ii) below are detailed in Mebius (2005) and (iii) is a consequence of (i) because the quaternion multiplication is associative.

Lemma 3.3. *Let $p = (p_1, p_2, p_3, p_4)^T \in \mathbb{S}^3$ and $q = (q_1, q_2, q_3, q_4)^T \in \mathbb{S}^3$ be arbitrary unit quaternions. Also consider arbitrary $R \in SO(4)$. Then the following hold.*

(i) *There are unique*

$$R_p^l = \begin{pmatrix} p_1 & -p_2 & -p_3 & -p_4 \\ p_2 & p_1 & -p_4 & p_3 \\ p_3 & p_4 & p_1 & -p_2 \\ p_4 & -p_3 & p_2 & p_1 \end{pmatrix} \in SO(4), \quad R_q^r = \begin{pmatrix} q_1 & -q_2 & -q_3 & -q_4 \\ q_2 & q_1 & q_4 & -q_3 \\ q_3 & -q_4 & q_1 & q_2 \\ q_4 & q_3 & -q_2 & q_1 \end{pmatrix} \in SO(4)$$

such that $p \cdot v = R_p^l v$ and $v \cdot q = R_q^r v$ for all $v \in \mathbb{S}^3$.

(ii) *There are, unique up to common sign change, unit quaternions $p_R, q_R \in \mathbb{S}^3$ such that $Rv = p_R \cdot v \cdot q_R$ for all $v \in \mathbb{S}^3$.*

(iii) *With the notation from (i), there is a smooth surjective group homomorphism*

$$\pi_{SO(4)} : \mathbb{S}^3 \times \mathbb{S}^3 \rightarrow SO(4), \quad (p, q) \mapsto R_p^l R_q^r = R_q^r R_p^l$$

with $\pi_{SO(4)}(p, q) = \pi_{SO(4)}(-p, -q)$.

Definition 3.4. *With an arbitrary right inverse $r_{SO(4)}$ of the double cover $\pi_{SO(4)} : \mathbb{S}^3 \times \mathbb{S}^3 \rightarrow SO(4)$ from Lemma 3.3, define $\Pi = (\pi, \pi) \circ r_{SO(4)} : SO(4) \rightarrow \mathcal{I}_0(G)$.*

The above map is well defined due to $\pi(x) = \pi(-x)$.

Theorem 3.5. *Consider curves $\gamma, \eta \in \mathcal{X}$ with arbitrary continuous lifts $\tilde{\gamma}, \tilde{\eta}$ and let L be defined as in (13) with a continuous loss function \tilde{L} , invariant under common sign changes. Then the following hold.*

(i) *For $(P, Q) \in \mathcal{I}_0(G)$ and arbitrary continuous lift $\widetilde{P\gamma Q}$ of $P\gamma Q$,*

(a) there is a unique $R \in SO(4)$ with the property

$$\widetilde{P\gamma Q}(t) = R\tilde{\gamma}(t) \text{ for all } t \in [0, 1], \quad (14)$$

(b) this satisfies $\Pi(R) = (P, Q)$.

$$(ii) \Pi\left(\operatorname{argmin}_{R \in SO(4)} \tilde{L}(R\tilde{\gamma}, \tilde{\eta})\right) = E_{\gamma, \eta} = \operatorname{argmin}_{P, Q \in SO(3)} L(P\gamma Q, \eta).$$

(iii) If \tilde{L} is additionally symmetric and $SO(4)$ -invariant then the inverse alignment property holds

$$(P, Q) \in E_{\gamma, \eta} \Leftrightarrow (P^{-1}, Q^{-1}) \in E_{P\gamma Q, \eta}$$

Asymptotic spatial alignment for two samples. Consider the $SO(4)$ invariant loss

$$\begin{aligned} \tilde{L}_2 : \mathcal{C}([0, 1], \mathbb{S}^3) \times \mathcal{C}([0, 1], \mathbb{S}^3) &\rightarrow \mathbb{R}_{\geq 0} \\ (\tilde{\gamma}, \tilde{\eta}) &\mapsto \int_0^1 \|\tilde{\gamma}(t) - \tilde{\eta}(t)\|^2 dt, \end{aligned} \quad (15)$$

which, via (13), induces the loss L_2 on \mathcal{X} .

Then, as in before Section 2.4, the minimization of $\tilde{L}_2(R\tilde{\gamma}, \tilde{\eta})$ over $R \in SO(4)$ is equivalent to maximizing $\operatorname{trace}(RH_{\tilde{\gamma}, \tilde{\eta}})$ with

$$H_{\tilde{\gamma}, \tilde{\eta}} = \int_0^1 \tilde{\eta}(t)\tilde{\gamma}(t)^T dt.$$

This is, again alluding to Umeyama (1991, Lemma, p. 377), solved by a SVD, from which, in conjunction with Theorem 3.5 we obtain at once the following.

Theorem 3.6. *Let $\gamma, \eta \in \mathcal{X}$ with arbitrary continuous lifts $\tilde{\gamma}, \tilde{\eta}$ to \mathbb{S}^3 and let L_2 be the loss on \mathcal{X} induced by \tilde{L}_2 through (13). Then, all elements in $E_{\gamma, \eta}$ are of the form $\Pi(USV^T)$, where $U, V \in O(4)$, together with $D = \operatorname{diag}(d_1, \dots, d_4)$, $d_1 \geq \dots \geq d_4 \geq 0$, are from a SVD, $H_{\tilde{\gamma}, \tilde{\eta}} = UDV^T$, and*

$$S = \begin{cases} I_{4 \times 4} & \text{if } \det(UV) = 1 \\ \operatorname{diag}(1, 1, 1, -1) & \text{if } \det(UV) = -1 \end{cases}.$$

If additionally $\operatorname{rank}(H_{\tilde{\gamma}, \tilde{\eta}}) > 2$, then $(P^*, Q^*) \in E_{\gamma, \eta}$ is unique.

Remark 3.7. *Note that $\operatorname{rank}(H_{\tilde{\gamma}, \tilde{\eta}})$ is independent of the particular choice of continuous lifts. Moreover in view of our two sample test, under the null hypothesis $\eta_0 = P\gamma_0 Q$ for some $P, Q \in SO(3)$, we have $H_{\tilde{\gamma}_0, \tilde{\eta}_0} = R$ with suitable $R \in SO(4)$ due (14), which has maximal rank.*

Theorem 3.8. *Assume $\gamma_1, \dots, \gamma_N \stackrel{i.i.d.}{\sim} \gamma$, $N \in \mathbb{N}$ and $\eta_1, \dots, \eta_M \stackrel{i.i.d.}{\sim} \eta$, $M \in \mathbb{N}$ are samples from GP models with center curves γ_0 and η_0 respectively, such that that their generating Gaussian processes fulfill Assumption (10) of Theorem 2.13. Further suppose that $\hat{\gamma}_N$ and $\hat{\eta}_M$, respectively, are pointwise measurable selections of the sample PEM curves. Denoting with $\tilde{\gamma}_0, \tilde{\gamma}_N, \tilde{\eta}_0, \tilde{\eta}_M$ arbitrary continuous lifts of $\gamma_0, \hat{\gamma}_N, \eta_0, \hat{\eta}_M$, under the additional assumption of $\operatorname{rank}(H_{\tilde{\gamma}_0, \tilde{\eta}_0}) > 2$, we have for every measurable selection $(\hat{P}_{N, M}, \hat{Q}_{N, M}) \in E_{\hat{\gamma}_N, \hat{\eta}_M}$ that*

$$\left(\hat{P}_{N, M}, \hat{Q}_{N, M}\right) \xrightarrow{N, M \rightarrow \infty} (P^*, Q^*) \text{ a.s.},$$

where (P^*, Q^*) is the unique element in E_{γ_0, η_0} .

Remark 3.9. *The only ingredient of the GP model needed in the proof of Theorem 3.8 is the uniform convergence of sample PEM curves to a unique population PEM. Moreover, in case of $\eta_0 = P\gamma_0 Q$ for $P, Q \in SO(3)$, due to Remark 3.7, the condition $\operatorname{rank}(H_{\tilde{\gamma}_0, \tilde{\eta}_0}) > 2$ is always fulfilled.*

4 Two Sample Permutation Tests

Among others, the following permutation tests are based on intrinsic loss functions from Definition 3.1 such that δ denotes either $\delta_{I,1}$, $\delta_{I,2}$ or δ_I .

Assume for the following that $\chi_1 = \{\gamma_1, \dots, \gamma_N\}$, $N \in \mathbb{N}$, and $\chi_2 = \{\eta_1, \dots, \eta_M\}$, $M \in \mathbb{N}$, denote samples of GP models with center curves γ_0 and η_0 respectively. By virtue of Corollary 2.14 we may assume that all of the following sample PEMs are unique elements in \mathcal{X} . We want to test

$$H_0 : \exists g \in \mathcal{S} : \eta_0 = g \cdot \gamma_0 \quad \text{vs.} \quad H_1 : \forall g \in \mathcal{S} : \eta_0 \neq g \cdot \gamma_0. \quad (16)$$

For a given significance level $\alpha \in (0, 1)$ we propose the following tests, first for $\mathcal{S} = 1$ (no group action), and then for $\mathcal{S} = \mathcal{I}_0(G) \times \text{Diff}^+[0, 1]$ (joint group action). Tests for other selections of the groups acting are similar.

Test 4.1 (No Group Action). *Let $\chi = \chi_1 \cup \chi_2$ be the pooled sample. Denote with $\chi_1^{(l)}$, $l \in \{1, \dots, \binom{N+M}{N}\}$, all possible choices with N elements from χ and with $\chi_2^{(l)}$ its complement in χ with M elements, such that $\chi_1^{(1)} = \chi_1$ and $\chi_2^{(1)} = \chi_2$. For each l compute the sample PEMs $t \mapsto \hat{\gamma}_{N,l}(t)$ of $\chi_1^{(l)}$ and $t \mapsto \hat{\eta}_{M,l}(t)$ of $\chi_2^{(l)}$, respectively, and compute $d_l = \delta(\hat{\gamma}_{N,l}, \hat{\eta}_{M,l})$.*

Setting $r = \#\{l \mid d_l > d_1\}$, reject the null hypothesis of equality of γ_0 and η_0 at significance level α if $r / \binom{N+M}{N} < \alpha$.

In order to include group actions, we modify Test 4.1 by first estimating the group element g via the following sample alignment procedure.

Procedure 4.2 (Sample Alignment: χ_1 to χ_2).

1. Compute the PESMs $\hat{\gamma}_N$ and $\hat{\eta}_M$ of χ_1 and χ_2 , respectively by Theorem 2.9.
2. Compute the spatial estimator $\hat{\psi} = (\hat{P}_\psi, \hat{Q}_\psi) \in E_{\hat{\gamma}_N, \hat{\eta}_M}$ from Theorem 3.6.
3. Compute the temporal estimator $\hat{\phi}$ from (11) for the curves $(\hat{\psi}, \text{id}_{[0,1]}) \cdot \hat{\gamma}_N$ and $\hat{\eta}_M$.
4. Define the new sample $\chi_1 = \{(\hat{\psi}, \hat{\phi}) \cdot \gamma_1, \dots, (\hat{\psi}, \hat{\phi}) \cdot \gamma_N\}$
5. Plug this into Step 1 and repeat Steps 2-5 until convergence of $\hat{\psi}$ and $\hat{\phi}$.
6. Return χ_1 as χ_1^{aligned} .

Test 4.3 (Joint Group Action with Preregistration). *Apply Test 4.1 to the aligned samples $(\hat{\psi}, \hat{\phi}) \cdot \chi_1$ and χ_2 where $(\hat{\psi}, \hat{\phi})$ has been determined by the Sample Alignment Procedure 4.2.*

Since extrinsic distances and the distance δ are minimized in the alignment, the δ -distance between χ_1^{aligned} and χ_2 tends to be smaller than that of permuted subsamples, giving Test 4.3 a level lower than α , cf. Table 1 (c). In order to keep the level, we perform alignment for each permutation.

Test 4.4 (Joint Group Action with Continual Registration). *Let $\chi = \chi_1 \cup \chi_2$ be the pooled sample. Denote with $\chi_1^{(l)}$, $l \in \{1, \dots, \binom{N+M}{N}\}$, all possible choices with N elements from χ and with $\chi_2^{(l)}$ its complement with M elements in χ such that $\chi_1^{(1)} = \chi_1$ and $\chi_2^{(1)} = \chi_2$.*

For $i, j \in \{1, 2\}$ let $\chi_{ij}^{(l)}$ denote the sample consisting of all trials of $\chi_i^{(l)}$ also belonging to χ_j . For each l , i compute the sample PEM $\hat{\eta}_{i,l}$ of $\chi_{i2}^{(l)}$.

For each i, l apply the Sample Alignment Procedure 4.2 to the two samples $\chi_{i1}^{(l)}$ and $\chi_{i2}^{(l)}$ to obtain the sample PEM $\hat{\gamma}_{i,l}^{\text{aligned}}$ of the aligned sample $\chi_{i1}^{(l)\text{aligned}}$. Compute the sample PEM $\hat{\omega}_{i,l}$ of the sample $\{\hat{\eta}_{i,l}, \hat{\gamma}_{i,l}^{\text{aligned}}\}$.

Apply the Sample Alignment Procedure 4.2 to the two single element samples $\hat{\omega}_{1,l}$ and $\hat{\omega}_{2,l}$ to obtain an aligned version $\hat{\omega}_{1,l}^{\text{aligned}}$ of $\hat{\omega}_{1,l}$ and compute $d_k = \delta(\hat{\omega}_{1,l}^{\text{aligned}}, \hat{\omega}_{2,l})$.

Letting $r = \#\{l \mid d_l > d_1\}$, reject the null hypothesis that there is $g \in \mathcal{S}$ such that $g \cdot \gamma_0 = \eta_0$ at significance level α if $r / \binom{N+M}{N} < \alpha$.

5 Simulations

GP models. The performance of our three tests for testing samples of GP models, with and without action of the group $\mathcal{I}_0(G)$, is studied using the following Gaussian processes

$$\begin{aligned}\varepsilon_t^1 &= a_1 \sin\left(\frac{\pi}{2}t\right) + a_2 \cos\left(\frac{\pi}{2}t\right) \\ \varepsilon_t^2 &= (\sin(4\pi t) + 1.5) \frac{\sum_{i=1}^{10} a_i \beta_i(x)}{\sqrt{\sum_{i=1}^{10} \beta_i(x)}}, \quad \beta_i(x) = e^{-\frac{(x - \frac{i-1}{9})^2}{0.2}}, \quad i = 1, \dots, 10\end{aligned}$$

and center curves $\gamma_0^\lambda(t)$, $\lambda \in \mathbb{R}$,

$$\begin{aligned}\alpha_x^\lambda(t) &= 80t^2 - 80t + 20 + \lambda \frac{e^{-\frac{1}{2}\left(\frac{t-0.5}{0.08}\right)^2}}{0.08\sqrt{2\pi}} - 35 \\ \alpha_y(t) &= 70t \sin(4\pi t^{0.7}) + 5 \\ \alpha_z(t) &= 10 \cos(13\pi),\end{aligned}$$

where $\alpha_x^\lambda, \alpha_y, \alpha_z$ are Euler angles of $\gamma_0^\lambda(t)$ measured in degrees. Then, five GP models are defined by

$$\begin{aligned}\gamma_A^0 &= \gamma_0^0(t) \text{Exp}\left(\iota((\varepsilon_{1,t}^1, \varepsilon_{2,t}^1, \varepsilon_{3,t}^1))\right) \\ \gamma_B^\lambda &= \gamma_0^\lambda(t) \text{Exp}\left(\iota\left(\begin{pmatrix} 1 & 0 & 0 \\ \frac{1}{2} & \frac{1}{2} & 0 \\ \frac{1}{\sqrt{3}} & \frac{1}{\sqrt{3}} & \frac{1}{\sqrt{3}} \end{pmatrix} (\varepsilon_{1,t}^2, \varepsilon_{2,t}^2, \varepsilon_{3,t}^2)^T\right)\right) \quad \text{for } \lambda \in \{0.5, 1, 2, 2.5\}.\end{aligned}\tag{17}$$

where $\varepsilon_{i,t}^j$, $i = 1, 2, 3$ and $j = 1, 2$, are independent realizations of ε_t^i .

Design of the simulation study. We consider γ and η each distributed according to one of the five GP models from (17) from which we simulate samples $\gamma_1, \dots, \gamma_N$ and η_1, \dots, η_N , $N \in \{10, 15, 30\}$, on $[0, 1]$ with an equidistant time grid of width $\Delta t = 0.01$. We call these *aligned samples* and we subject the resulting $N(N+1)/2$ pairings to Test 4.1, cf. Table 1 (a). Further for fixed rotations $P \in SO(3)$ with Euler angles $\alpha_x = -0.5^\circ$, $\alpha_y = 13^\circ$, $\alpha_z = -9^\circ$ and $Q \in SO(3)$ with Euler angles $\alpha_x = 12^\circ$, $\alpha_y = 0^\circ$, $\alpha_z = 5^\circ$ we misalign each sample η_1, \dots, η_N to obtain $\tilde{\eta}_1, \dots, \tilde{\eta}_N$ via $\tilde{\eta}_n = P\eta_n Q$ ($n = 1, \dots, N$). We call these the *misaligned samples* and we subject the resulting $N(N+1)/2$ pairings to Tests 4.1, 4.3 and 4.4, cf. Table 1 (b), (c) and (d).

We use $M = 2000$ simulations and for each $M_{perm} = 5000$ permutations. We do not simulate time warping actions because, in contrast to spatial alignment which can be explicitly estimated via a SVD, running for every permutation for every simulation the dynamic program from Section 3.1 would require in our implementation 70.000 hours on an Intel(R) Core(TM) i5-4300U CPU with 1.90GHz.

Results of the simulation study. In Table 1 we report the corresponding acceptance rates. Subtracting the diagonal elements from one gives the type I errors, the off-diagonals give type II errors. For aligned samples, Test 4.1 keeps the level (Table 1 (a)) and so does Test 4.4 for misaligned data (Table 1 (d)). For misaligned data, Test 4.1 completely fails to identify equality up to the spacial action (Table 1 (b)) while Test 4.3 (Table 1 (c)) masters identification but at a lower level, at the price of a lower power. We have also applied Test 4.4 to aligned data which gives a table similar to Table 1 (d).

6 Applications To Gait Data

In this application we study biomechanical gait data collected for an experiment performed in the School of Rehabilitation Science (McMaster University, Canada). In order to identify individual

$\begin{matrix} 10 \\ N=15 \\ 30 \end{matrix}$	γ_A^0	$\gamma_B^{0.5}$	γ_B^1	γ_B^2	$\gamma_B^{2.5}$
γ_A^0	95.8 94.5 94.5	80.7 72.8 45.1	29.8 8.6 0.0	0.0 0.0 0.0	0.0 0.0 0.0
$\gamma_B^{0.5}$		95.4 94.6 94.8	88.1 81.6 63.0	8.4 0.2 0.0	0.1 0.0 0.0
γ_B^1			94.2 95.3 93.65	49.7 26.4 0.3	7.1 0.3 0.0
γ_B^2				95.3 95.3 95.4	87.9 81.2 61.8
$\gamma_B^{2.5}$					95.3 95.2 95.4

(a) Test 4.1 on aligned samples.

$\begin{matrix} 10 \\ N=15 \\ 30 \end{matrix}$	γ_A^0	$\gamma_B^{0.5}$	γ_B^1	γ_B^2	$\gamma_B^{2.5}$
γ_A^0	0.0 0.0 0.0	0.0 0.0 0.0	0.0 0.0 0.0	0.0 0.0 0.0	0.0 0.0 0.0
$\gamma_B^{0.5}$		0.0 0.0 0.0	0.0 0.0 0.0	0.0 0.0 0.0	0.0 0.0 0.0
γ_B^1			0.0 0.0 0.0	0.0 0.0 0.0	0.0 0.0 0.0
γ_B^2				0.0 0.0 0.0	0.0 0.0 0.0
$\gamma_B^{2.5}$					0.0 0.0 0.0

(b) Test 4.1 on misaligned samples.

$\begin{matrix} 10 \\ N=15 \\ 30 \end{matrix}$	γ_A^0	$\gamma_B^{0.5}$	γ_B^1	γ_B^2	$\gamma_B^{2.5}$
γ_A^0	99.9 99.9 99.9	93.6 90.2 73.1	50.1 16.5 0.0	0.0 0.0 0.0	0.0 0.0 0.0
$\gamma_B^{0.5}$		96.1 95.9 96.5	93.1 88.4 75.9	11.5 0.8 0.0	0.2 0.0 0.0
γ_B^1			95.8 96.8 96.1	63.4 39.0 0.8	12.4 0.3 0.0
γ_B^2				96.4 96.6 96.3	91.7 89.1 75.1
$\gamma_B^{2.5}$					96.7 96.4 97.1

(c) Test 4.3 on misaligned samples.

$\begin{matrix} 10 \\ N=15 \\ 30 \end{matrix}$	γ_A^0	$\gamma_B^{0.5}$	γ_B^1	γ_B^2	$\gamma_B^{2.5}$
γ_A^0	94.9 94.9 95.4	81.8 74.0 40.0	24.1 2.8 0.0	0.0 0.0 0.0	0.0 0.0 0.0
$\gamma_B^{0.5}$		95.3 95.2 94.3	89.3 86.1 70.5	9.4 0.2 0.0	0.0 0.0 0.0
γ_B^1			95.1 95.3 95.8	59.7 30.2 0.4	8.0 0.2 0.0
γ_B^2				95.2 94.9 95.0	89.1 85.4 67.8
$\gamma_B^{2.5}$					95.7 94.8 95.0

(d) Test 4.4 on misaligned samples.

Table 1: Average acceptances rate in percent over $M = 2000$ simulations, testing (16).

gait patterns in a common practice clinical setting, subjects walked along a 10 m pre-defined straight path at comfortable speed. Retro-reflective markers were placed by an experienced technician onto identifiable skin locations on the upper and lower leg, following a standard protocol. Eight cameras recorded the position of these markers and from these spatial marker motions, a moving orthogonal frame $E_u(t) \in SO(3)$ describing the rotation of the upper leg w.r.t. the laboratory's fixed coordinate system was determined, and one for the lower leg, $E_l(t) \in SO(3)$, each of which was aligned near $I_{3 \times 3}$ when the subject stood straight.

Eight subjects repeatedly walked along the straight path and for each walk a single gait cycle $\gamma(t) = E_u(t)E_l(t)^T$ representing the motion of the upper leg w.r.t. the lower leg was recorded. Due to Newton's law, these curves are continuously differentiable, i.e., $\gamma \in \mathcal{X}$. By design each subject started walking about three gait cycles prior to data collection allowing the assumption of independence of recorded gait cycles. Two samples ("before" and "after" marker replacement) of $N \approx 12$ walks were available for analysis.

Replacing markers between sessions results then in fixed and different rotations of the upper and lower legs conveyed by suitable $P, Q \in SO(3)$ such that $E'_u(t) = PE_u(t)$ and $E'_l(t) = Q^T E_l(t)$. In consequence of Lemma 2.1, marker replacement corresponds to the action of $\mathcal{I}_0(G)$ on gait curves in \mathcal{X} ,

$$\gamma'(t) = E'_u(t)E'_l(t)^T = P\gamma(t)Q.$$

Although, P and Q are near $I_{3 \times 3}$, it has been known (see Noehren et al. (2010) and Groen et al. (2012)) that this *marker replacement effect* makes identification of individual gait patterns challenging. This is illustrated in Figure 1a: While the effect is small on the dominating Euler flexion-extension angle, it can amount to a considerable distortion of other angles; here the Euler internal-external angle is mainly shifted.

Indeed, applying Test 4.1 to the gait samples before and after marker replacement shows that 6 out of 8 subjects cannot be identified with significance level $\alpha = 5\%$, cf. Table 2a. If, however, the group action due to $\mathcal{I}_0(G)$, which precisely models the marker replacement effect, is taken

(a) Test 4.1 without any spatial and temporal alignment.

Vol	1	2	3	4	5	6	7	7
1	0.6	0	0	0	0	0	0	0
2	0	0.0	0	0	0	0	0	0
3	0	0	2.7	0	0	0	0	0
4	0	0	0	0.1	0	0	0	0
5	0	0	0	0	0.0	0	0	0
6	0	0	0	0	0	6.5	0	0
7	0	0	0	0	0	0	6.8	0
8	0	0	0	0	0	0	0	1.6

(b) Test 4.4 including spatial and temporal alignment.

Vol	1	2	3	4	5	6	7	7
1	23.6	0	0	0	0	0	0	0
2	0	39.2	0	0	0	0	0	0
3	0	0	66.3	0	0	0	0	0
4	0	0	0	53.8	0	0	0	0
5	0	0	0	0	6.2	0	0	0
6	0	0	0	0	0	53.7	0	0
7	0	0	0	0	0	0	97.2	0
8	0	0	0	0	0	0	0	60.7

Table 2: Displaying p -values in percentage of permutation tests of equality of means before and after marker replacement for different volunteers.

into account in addition with sample-wise time warping, by Test 4.4, then all 8 subjects can be reliably identified and well discriminated from other subjects, cf. Table 2b. This preliminary study warrants larger investigations to develop a protocol allowing for inferential gait analysis robustly modeling marker replacement and temporal warping effects.

Acknowledgment

The first and the last author gratefully acknowledge DFG HU 1575/4 and the Niedersachsen Vorab of the Volkswagen Foundation.

A Appendix: Proofs

For convenience, here we will always use $I = [0, 1]$.

Proof of Lemma 2.1. Using (Helgason 1962, Theorem 4.1(i) on p. 207), we have to assert that $\mathcal{G} := G \times G$ and $\mathcal{K} := \text{diag}(G \times G)$ form a *Riemannian symmetric pair* where \mathcal{G} is semisimple and acts effectively on $\mathcal{G}/\mathcal{K} = \{[g, h] : g, h \in G\}$, $[g, h] = \{(gk, hk) : k \in G\}$. Here the action is given by $(g', h') : [g, h] \mapsto [g'g, h'h]$. The fact that $(\mathcal{G}, \mathcal{K})$ is a Riemannian symmetric pair is asserted in (Helgason 1962, p. 207), $G = SO(3)$ is simple, hence semisimple and the effective action follows from the fact \mathcal{G} has no trivial normal divisors $N \subset \mathcal{K}$, cf. (Helgason 1962, p. 110). For if $\{(e, e)\} \neq N \subset \mathcal{K}$ would be a normal divisor of \mathcal{G} then there would be a subgroup $\{e\} \neq H$ of G with the property that for every $h \in H, g, k \in G$, in particular for $g \neq k$, there would be $h' \in H$ such that

$$(g, k)(h, h)(g^{-1}, k^{-1}) = (h', h'),$$

i.e. $k^{-1}g$ would be in the center of G , which, however, is trivial because G is non-commutative and simple. Hence $g = k$, a contradiction. \square

Proof of Theorem 2.5. In the following we set $\|C_t\|_\infty = \max_{t \in I} \|C_t\|$, for short.

First observe that (3) and (7) imply

$$\delta_0(t)^T \text{Exp}(\iota \circ C_t) \delta_0(t) \text{Exp}(\iota \circ D_t) = \text{Exp}\left(\iota \circ (\delta_0(t)^T C_t)\right) \text{Exp}(\iota \circ D_t).$$

Thus, since $\|\delta_0(t)^T C_t\|_\infty = \|C_t\|_\infty = \mathcal{O}_p(\sigma)$, we may w.l.o.g. set $\delta_0(t) = I_{3 \times 3}$ for all $t \in I$.

Next, define the group and vector valued processes

$$h_t = \text{Exp}(\iota \circ C_t) \text{Exp}(\iota \circ D_t), \text{ and } H_t = \iota^{-1} \circ \text{Exp}|_{\mathfrak{g}}^{-1} h_t,$$

where $\mathcal{B}_\pi(0) \subset \mathfrak{V} \subset \mathbb{R}^3$ is a set making the Lie exponential restricted to \mathfrak{V} bijective onto G . In consequence, setting $A_t = C_t + D_t$ and

$$\tilde{A}_t = H_t - A_t,$$

we have

$$\text{Exp}(\iota \circ A_t + \iota \circ \tilde{A}_t) = \text{Exp}(\iota \circ C_t) \text{Exp}(\iota \circ D_t),$$

and in order to prove the theorem, it suffices to show that for all $\epsilon > 0$ there is $M = M_\epsilon > 0$ such that

$$\mathbb{P}\left\{\sigma^{-2}\|\tilde{A}_t\|_\infty > M\right\} < \epsilon. \quad (18)$$

To this end, fix $\epsilon > 0$ and consider the function

$$f : \mathfrak{so}(3) \times \mathfrak{so}(3) \rightarrow \mathfrak{so}(3), (X, Y) \mapsto \text{Log}(\text{Exp}(X) \text{Exp}(Y))$$

which is well-defined and analytic in a neighborhood U of $(0, 0) \in \mathfrak{so}(3) \times \mathfrak{so}(3)$. In particular, there is a compact subset $K \subset U$ which contains a neighborhood of $(0, 0)$ such that the Taylor expansion

$$f(X, Y) = X + Y + \mathcal{O}(\|X\|^2 + \|Y\|^2) \quad (19)$$

is valid for all $(X, Y) \in K$.

We now split the l.h.s. of (18) into the two summands

$$\mathbb{P}\{\mathfrak{K}; \sigma^{-2}\|\iota^{-1} \circ \text{Log}(h_t) - C_t - D_t\|_\infty > M\} \text{ and } \mathbb{P}\{\mathfrak{K}^C; \sigma^{-2}\|H_t - C_t - D_t\|_\infty > M\},$$

where $\mathfrak{K} = \{\omega \in \Omega \mid \forall t \in I : (\iota \circ C_t, \iota \circ D_t) \in K\}$. Note that we used in the first summand that $\iota \circ \text{Log}(h_t) = H_t$ for all $t \in I$, if the complete sample path $t \mapsto (\iota \circ C_t, \iota \circ D_t)$ is contained in K .

For the first summand we have $\omega \in \mathfrak{K}$ and Taylor's formula (19) is applicable, yielding

$$\|\tilde{A}_t\|_\infty \leq \Lambda \max_{t \in I} (\|C_t\|^2 + \|D_t\|^2) \leq \Lambda \|C_t\|_\infty^2 + \Lambda \|D_t\|_\infty^2,$$

where $\Lambda \geq 0$ can be chosen independent of $t \in I$, since the Hessian of f is bounded on K . Thus, $\max_{t \in I} \|\tilde{A}_t\| = \mathcal{O}_p(\sigma^2)$ on \mathfrak{K} and therefore we find $M > 0$ such that

$$\mathbb{P}\{\mathfrak{K}; \sigma^{-2}\|\iota^{-1} \circ \text{Log}(h_t) - C_t - D_t\|_\infty \geq M\} < \frac{\epsilon}{2}, \quad (20)$$

The second summand is characterized by the fact that there is $t \in I$ with $(\iota \circ C_t, \iota \circ D_t) \notin K$. Since $\|C_t\|_\infty, \|D_t\|_\infty \xrightarrow{\mathbb{P}} 0$, it follows that $\mathbb{P}(\mathfrak{K}^C) \rightarrow 0$ as $\sigma \rightarrow 0$. Hence there is $\sigma_0 > 0$ such that for all $\sigma < \sigma_0$,

$$\mathbb{P}(\mathfrak{K}^C) < \frac{\epsilon}{2}.$$

In consequence, for any $M > 0$ and all $\sigma < \sigma_0$,

$$\mathbb{P}\{\mathfrak{K}^C; \sigma^{-2}\|H_t - C_t - D_t\|_\infty > M\} \leq \mathbb{P}\{(\iota \circ C_t, \iota \circ D_t) \in K^C \text{ for some } t \in I\} < \frac{\epsilon}{2}.$$

In conjunction with (20), this yields (18) completing the proof. \square

Proof of Theorem 2.9. (i) follows at once from the arguments preceding the theorem. To see (ii) we note that the sum of \mathcal{C}^1 functions is again \mathcal{C}^1 and the derivative of the expected value is the expected value of derivatives in case of dominated convergence of the derivative. Now consider $\Gamma = \{\mathbb{E}[\gamma(t)] : t \in [0, 1]\}$, $\Gamma_N = \{\bar{\gamma}_N(t) : t \in [0, 1]\}$ and $\mathcal{F} = \{B \in \mathbb{R}^{3 \times 3} : \text{rank}(B) \leq 1\}$. Because Γ and Γ_N are compact and \mathcal{F} is closed, in case of uniqueness there are open sets $U \supset \Gamma$, $U_N \supset \Gamma_N$ such that $U \cap \mathcal{F} = \emptyset = U_N \cap \mathcal{F}$. By Dudek and Holly (1994, Theorem 4.1, p. 6), $\text{pr}|_U$ and $\text{pr}|_{U_N}$ are even analytic, yielding that the composition is \mathcal{C}^1 as claimed. \square

Lemma A.1. *Suppose that the distribution of a random variable $X \in \mathbb{R}^3$ with existing first moment $\mathbb{E}[X]$ is even, i.e., that $\mathbb{P}\{X \in M\} = \mathbb{P}\{-X \in M\}$ for all Borel sets $M \subset \mathbb{R}^3$ and $\mathbb{E}[\cos \|X\|] > 0$. Then $\mathbb{E}[\text{Exp}(\iota \circ X)]$ is symmetric positive definite.*

Proof. With the Rodriguez formula (4) we have

$$\begin{aligned} \text{Exp}(\iota \circ X) &= I_{3 \times 3} + \iota \circ X \text{sinc}\|X\| + (\iota \circ X)^2 \frac{1 - \cos\|X\|}{\|X\|^2} \\ &= \cos(\|X\|)I_{3 \times 3} + \iota \circ X \text{sinc}\|X\| + (1 - \cos(\|X\|)) \frac{XX^T}{\|X\|^2}, \end{aligned}$$

where the second equality is due to

$$\left(\iota \left(\frac{X}{\|X\|} \right) \right)^2 = \frac{XX^T}{\|X\|^2} - I_{3 \times 3}.$$

By hypothesis, X is even, hence $\mathbb{E}[\iota \circ X \text{sinc}\|X\|] = \iota \circ \mathbb{E}[X \text{sinc}\|X\|] = 0$ which yields that

$$\mathbb{E}[\text{Exp}(\iota \circ X)] = \mathbb{E}[\cos\|X\|]I_{3 \times 3} + \mathbb{E}\left[(1 - \cos\|X\|) \frac{XX^T}{\|X\|^2} \right]$$

is symmetric. Let $V \in \mathbb{R}^3$ be arbitrary with $\|V\| = 1$, then positive definiteness follows from the inequality

$$V^T \mathbb{E}[\text{Exp}(\iota \circ X)] V = \mathbb{E}[\cos\|X\|] + \mathbb{E}\left[(1 - \cos\|X\|) \frac{(V^T X)^2}{\|X\|^2} \right] \geq \mathbb{E}[\cos\|X\|] > 0.$$

□

Proof of Theorem 2.10. Fixing $t \in I$ and letting $\mathbb{E}[\gamma(t)] = UDV^T$ be a SVD, with Theorem 2.9, we need to assert $\gamma_0(t) = USV^T$. Since $\mathbb{E}[\gamma(t)] = \gamma_0(t)\mathbb{E}[\text{Exp}(\iota \circ A_t)]$, this holds if $\mathbb{E}[\text{Exp}(\iota \circ A_t)]$ is symmetric and positive definite.

Indeed, let $\mathbb{E}[\text{Exp}(\iota \circ A_t)] = \tilde{V}\Lambda\tilde{V}^T$ with $\tilde{V} \in SO(3)$ and diagonal $\Lambda > 0$. Then $\Lambda = D$ (assuming that the singular values are sorted non increasingly), giving

$$UDV^T = \gamma_0(t)\tilde{V}D\tilde{V}^T.$$

Since the eigenspaces corresponding to same eigenvalues spanned by the columns of \tilde{V} and V agree, we can choose $\tilde{V} = V$, yielding $\gamma_0 = UV^T$ with $U \in SO(3)$, since $U = \gamma_0(t)\tilde{V} \in SO(3)$, which proves the assertion, even with $S = I_{3 \times 3}$.

With Lemma A.1 it remains to prove that $A_t = X \sim \mathcal{N}(0, \Sigma)$ in \mathbb{R}^3 fulfills $\mathbb{E}[\cos\|X\|] > 0$. Indeed, making use of the Fourier transformation of Gaussian densities in the 3rd equality below, we have

$$\begin{aligned} \mathbb{E}[\cos\|X\|] &= \frac{1}{(2\pi)^{k/2} \sqrt{\nu_1 \cdots \nu_k}} \int_{\mathbb{R}^k} e^{-y^T \tilde{\nu}^{-1} y / 2} \cos(\|y\|) dy \\ &= \frac{1}{(2\pi)^{k/2}} \int_{S^{k-1}} \left(\int_0^\infty e^{-r^2/2} \cos\left(r\sqrt{\phi^T \tilde{\nu} \phi}\right) dr \right) d\sigma(\phi) \\ &= \frac{1}{(2\pi)^{k/2-1}} \int_{S^{k-1}} \frac{1}{2} e^{-\phi^T \tilde{\nu} \phi / 2} d\sigma(\phi) > 0, \end{aligned}$$

with the spherical volume element $d\sigma(\phi)$ on the $k - 1$ dimensional unit sphere S^{k-1} . Here we have used a svd $\Sigma = W \text{diag}(\nu_1, \nu_2, \nu_3) W^T$ with $W = (w_1, w_2, w_3) \in SO(3)$, the smallest index $k \in \{1, 2, 3\}$ such that $\nu_k > 0$, $\tilde{\nu} = \text{diag}(\nu_1, \dots, \nu_k)$ and $y = (w_1, \dots, w_k)^T x \in \mathbb{R}^k$. □

Proof of Corollary 2.12. That the extrinsic sample mean set is a strongly consistent estimator of the extrinsic population mean set follows from a more general result by Ziezold (1977). In case of uniqueness, guaranteed by the model we have that the center curve and PEM agree by virtue of Theorem 2.10. Hence, every measurable selection of the sample mean converges almost surely to the unique population mean yielding the assertion (see also Bhattacharya and Patrangenaru (2003)). \square

Proof of Theorem 2.13. First, we claim that in order to prove (i) it suffices to show that

$$\max_{t \in I} \|\bar{\gamma}_N(t) - \mathbb{E}[\gamma(t)]\| \rightarrow 0 \quad a.s. \quad (21)$$

Indeed, by Theorem 2.10 the PEM of γ is unique and in conjunction with the proof of Theorem 2.9 and the notation there, there is $\varepsilon_0 > 0$ such that

$$\|\mathbb{E}[\gamma(t)] - \mathcal{F}\| \geq \varepsilon_0, \text{ for all } t \in I. \quad (22)$$

Now, if (21) is true, there is a measurable set $\tilde{\Omega}$ with $\mathbb{P}(\tilde{\Omega}) = 1$ such that for every $\omega \in \tilde{\Omega}$ there is $N_\omega(\varepsilon_0) \in \mathbb{N}$ such that for all $N \geq N_\omega(\varepsilon_0)$ we have that

$$\|\bar{\gamma}_N(\omega, t) - \mathbb{E}[\gamma(t)]\| < \frac{\varepsilon_0}{2}$$

for all $t \in I$. This implies that $\bar{\gamma}_N(t) \notin \mathcal{F}$ for all $t \in I$, since

$$\|\bar{\gamma}_N(t) - \mathcal{F}\| \geq \|\mathbb{E}[\gamma(t)] - \mathcal{F}\| - \|\bar{\gamma}_N(t) - \mathbb{E}[\gamma(t)]\| > \frac{\varepsilon_0}{2}$$

for all $t \in I$ and all $N > N_\omega(\varepsilon_0)$. Therefore, $\hat{E}_N(t)$ is a unique point $\hat{\mu}_N(t)$ for all $N > N_\omega(\varepsilon_0)$. Arguing as in the proof of (ii) of Theorem 2.9, we conclude $\hat{\mu}_N \in \mathcal{X}$.

Thus, it remains to prove the uniform convergence (21). By Davidson (1994, Theorem 21.8) it suffices to show that the sequence of processes $\bar{\gamma}_N(t)$ is stochastically equicontinuous, since we already have pointwise convergence by Corollary 2.12.

In order to establish this, consider $\gamma_n(t) = \gamma_0(t)\text{Exp}(\iota \circ A_t^n)$ with $A_t^n \sim A_t$ for $n = 1, \dots, N$. Define Ω' with $\mathbb{P}(\Omega') = 1$ by $\Omega' = \bigcap_{n \in \{1, \dots, N\}} \Omega_n$, where Ω_n is the set for which $A^n(\omega) \in \mathcal{C}^1(I, \mathbb{R}^3)$. Using that γ_0 and $A^n(\omega)$ are Lipschitz continuous with Lipschitz constants $\max_{t \in I} \|\gamma_0'(t)\|$ and $L_{A^n}(\omega) = \max_{t \in I} \|\partial_t A_t^n(\omega)\|$, respectively, we obtain for all $\omega \in \Omega'$

$$\begin{aligned} & \|\gamma_0(s)\text{Exp}(\iota \circ A_s^n(\omega)) - \gamma_0(t)\text{Exp}(\iota \circ A_t^n(\omega))\| \\ & \leq \|\gamma_0(s) - \gamma_0(t)\| \|\text{Exp}(\iota \circ A_s^n(\omega))\| + \|\gamma_0(t)\| \|\text{Exp}(\iota \circ A_s^n(\omega)) - \text{Exp}(\iota \circ A_t^n(\omega))\| \\ & \leq M(1 + L_{A^n}(\omega))|s - t|, \end{aligned}$$

with $M > 0$ sufficiently large because Exp is Lipschitz continuous as well. In consequence, the triangle inequality then yields

$$\begin{aligned} \|\bar{\gamma}_N(\omega, s) - \bar{\gamma}_N(\omega, t)\| & \leq \frac{1}{N} \sum_{n=1}^N \|\gamma_0(s)\text{Exp}(\iota \circ A_s^n(\omega)) - \gamma_0(t)\text{Exp}(\iota \circ A_t^n(\omega))\| \\ & \leq M \left(1 + \frac{1}{N} \sum_{n=1}^N L_{A^n}(\omega) \right) |s - t| \end{aligned} \quad (23)$$

for all $\omega \in \Omega'$.

In conjunction with the strong law,

$$\frac{1}{N} \sum_{n=1}^N L_{A^n}(\omega) \rightarrow \mathbb{E} \left[\max_{t \in I} \|\partial_t A_t\| \right] \text{ as } N \rightarrow \infty$$

for all $\omega \in \Omega$ except for a null set, and Assumption (10), guaranteeing boundedness of the above r.h.s., (23) yields stochastic equicontinuity, finishing the proof of (i).

(ii): Recalling (22) define the compact set

$$K = \overline{\bigcup_{t \in I} \left\{ B \in \mathbb{R}^{3 \times 3} \mid \|\mathbb{E}[\gamma(t)] - B\| < \frac{\varepsilon_0}{2} \right\}},$$

which satisfies $K \cap \mathcal{F} = \emptyset$. Again by Dudek and Holly (1994, Theorem 4.1, p. 6) we have that $\mathbf{pr}|_K$ is analytic and hence Lipschitz continuous.

Since we proved in (i) that $\bar{\gamma}_N$ converges a.s. uniformly to $\mathbb{E}[\gamma]$, a.s. for $\omega \in \Omega$ there is $N_K(\omega)$ such that $\bar{\gamma}_N \in K$ for all $N > N_K(\omega)$. Thus, by Lipschitz continuity of $\mathbf{pr}|_K$,

$$\|\hat{\mu}_N(t) - \gamma_0(t)\| = \|\mathbf{pr}(\bar{\gamma}_N(t)) - \mathbf{pr}(\mathbb{E}[\gamma(t)])\| \leq C_K \|\bar{\gamma}_N(t) - \mathbb{E}[\gamma(t)]\| \quad (24)$$

for $C_K > 0$ sufficiently large and all $N > N_K(\omega)$, a.s. for $\omega \in \Omega$. Now, the a.s. uniform convergence $\bar{\gamma}_N \rightarrow \mathbb{E}[\gamma]$ implies the a.s. uniform convergence of the left hand side of (24) to zero, yielding (ii), in conjunction with (5). \square

Proof of Corollary 2.14. Using the notation of the proof of Theorem 2.13, with ε_0 there and any $0 < \varepsilon < \varepsilon_0$, we have with Theorem 2.9 that

$$\begin{aligned} \mathbb{P}\{t \mapsto \hat{\mu}_N(t) \in \mathcal{X}\} &\geq \mathbb{P}\left\{\max_{t \in I} \|\bar{\gamma}_N(t) - \mathcal{F}\| > \varepsilon\right\} \\ &\geq \mathbb{P}\left\{\max_{t \in I} \|\bar{\gamma}_N(t) - \mathbb{E}[\gamma(t)]\| < \varepsilon_0 - \varepsilon\right\} \geq 1 - \frac{\mathbb{E}\left[\max_{t \in I} \|\bar{\gamma}_N(t) - \mathbb{E}[\gamma(t)]\|\right]}{\varepsilon_0 - \varepsilon}. \end{aligned} \quad (25)$$

In conjunction with (21) and $\|\bar{\gamma}_N(t) - \mathbb{E}[\gamma(t)]\| \leq \sqrt{6}$ for all $t \in I$ (recall that $\|P\| = \sqrt{3/2}$ for all $P \in SO(3)$), Lebesgue's dominated convergence theorem yields

$$\mathbb{E}\left[\max_{t \in I} \|\bar{\gamma}_N(t) - \mathbb{E}[\gamma(t)]\|\right] \rightarrow 0, \quad \text{for } N \rightarrow \infty,$$

which together with inequality (25) implies the assertion of the corollary. \square

Proof of Theorem 3.2. We consider $\delta = \delta_{I,1}$, the proof for the other two losses is similar.

(i): Given two curves $\gamma, \eta \in \mathcal{X}$, the length $\delta(\gamma, \eta)$ of the curve $t \mapsto \zeta(t) = \gamma(t)\eta(t)^{-1}$ based on the intrinsic distance $d_{SO(3)}$ on $SO(3)$ has the representation

$$\sup \left\{ \sum_{k=0}^{K-1} d_{SO(3)}(\zeta(t_k), \zeta(t_{k+1})) \mid K \in \mathbb{N}, 0 = t_0 < t_1 < \dots < t_{K-1} < t_K = 1 \right\},$$

where (5) implies $d_{SO(3)}(\zeta(t_k), \zeta(t_{k+1})) = d_{SO(3)}(\zeta(t_k)^{-1}, \zeta(t_{k+1})^{-1})$ yielding symmetry of δ .

(ii) follows directly from biinvariance and from the fact that the length of a curve does not depend on its parametrization.

(iii): $\delta(P\gamma, \eta) = \delta(\gamma, \eta)$ is again a direct consequence of the biinvariance of the metric.

(iv): Assume $\eta = P\gamma$. Then by (iii) we have

$$\delta(\gamma, \eta) = \delta(\gamma, P\gamma) = \delta(\gamma, \gamma) = \text{length}(\gamma\gamma^{-1}) = 0.$$

For the other way round assume that $\delta(\gamma, \eta) = 0$. In consequence, $\gamma\eta^{-1}$ is a constant, $P^{-1} \in SO(3)$, say, yielding $P\gamma = \eta$. The proof of (v) is straightforward. \square

Proof of Theorem 3.5. Let $\gamma \in \mathcal{X}$ and $(P, Q) \in SO(3) \times SO(3)$ be arbitrary and choose continuous lifts $\tilde{\gamma}$ and $\widetilde{P\gamma Q}$ of γ and $P\gamma Q$. Since π is a homomorphism, we have that

$$\pi(p\tilde{\gamma}q) = \pi\left(\widetilde{P\gamma Q}\right)$$

with any $p \in \pi^{-1}(P)$ and $q \in \pi^{-1}(Q)$. Since π is a double cover, there is a function $\epsilon : [0, 1] \rightarrow \{-1, 1\}$ such that

$$p\tilde{\gamma}q = \epsilon\widetilde{P\gamma Q}.$$

By continuity of the lifts, ϵ must be constant and hence by virtue of (iii) of Lemma 3.3 there is a unique $R \in SO(4)$ such that $R\tilde{\gamma} = \epsilon p\tilde{\gamma}q = \widetilde{P\gamma Q}$ yielding assertion (i),(a). Then $(\pi, \pi) \circ r_{SO(4)} R = (\pi, \pi)(\kappa(p, q)) = (P, Q)$ with $\kappa \in \{-1, 1\}$ yields assertion (i),(b).

Assertion (ii) follows at once from the following

$$\min_{P, Q \in SO(3)} L(P\gamma Q, \eta) \geq \min_{R \in SO(4)} \tilde{L}(R\tilde{\gamma}, \tilde{\eta}) \geq \min_{P, Q \in SO(3)} \tilde{L}\left(\widetilde{P\gamma Q}, \tilde{\eta}\right) \geq \min_{P, Q \in SO(3)} L(P\gamma Q, \eta).$$

Here the first inequality is due to the definition (taking into account that $-I_{4 \times 4} \in SO(4)$),

$$L(P\gamma Q, \eta) = \min \left\{ \tilde{L}\left(\widetilde{P\gamma Q}, \tilde{\eta}\right), \tilde{L}\left(-\widetilde{P\gamma Q}, \tilde{\eta}\right) \right\},$$

and (i),(a); the second follows from the consideration that for any $R \in SO(4)$ we have $\pi(R\tilde{\gamma}) = P\gamma Q$ with $(P, Q) = \Pi(R)$, such that a continuous lift can be chosen such that $\widetilde{P\gamma Q} = R\tilde{\gamma}$; and the third holds again due to the definition of \tilde{L} .

Assertion (iii) is straightforward. \square

Proof of Theorem 3.8. Consider the function

$$f : \mathbb{X} \times \mathbb{Y} \rightarrow \mathbb{R}, \left((P, Q), (\gamma_1, \gamma_2) \right) \mapsto L(P\gamma_1 Q, \gamma_2)$$

mapping from the compact space $\mathbb{X} = \mathcal{I}_0(G)$ and $\mathbb{Y} = \mathcal{X} \times \mathcal{X}$. By hypothesis and Theorem 3.6, for fixed $y_0 = (\gamma_0, \eta_0)$ it has a unique minimizer $x^* = (P^*, Q^*) \in \mathbb{X}$. Moreover, by Theorem 2.13, for any sample PEM curves, $y = (\hat{\gamma}_N, \hat{\eta}_M)$ converges to y_0 outside a set of measure zero and both sample PEM curves belong a.s. eventually to \mathcal{X} by Corollary 2.14. By Lemma A.2 below (in Chang (1986, Lemma 2)), every minimizer $x = (\hat{P}_N, \hat{Q}_M)$ of $f((P, Q), (\hat{\gamma}_N, \hat{\eta}_M))$ converges to $x^* = (P^*, Q^*)$, again outside a set of measure zero. \square

Lemma A.2. *Let $f : \mathbb{X} \times \mathbb{Y} \rightarrow \mathbb{R}$ be continuous with \mathbb{X} compact, and assume for fixed $y_0 \in \mathbb{Y}$ that $x \mapsto f(x, y_0)$ has a unique minimizer x^* . Moreover suppose that y_n converges to y_0 and that each x_n is a minimizer of $x \mapsto f(x, y_n)$. Then $x_n \rightarrow x^*$.*

Proof. By compactness, x_n has cluster points. Since by hypothesis $f(x_n, y_n) \leq f(x, y_n)$ for all $n \in \mathbb{N}$ and $x \in \mathbb{X}$, by continuity and uniqueness, every cluster point is x^* . \square

References

- Amor, B. B., J. Su, and A. Srivastava (2016). Action recognition using rate-invariant analysis of skeletal shape trajectories. *Pattern Analysis and Machine Intelligence, IEEE Transactions on* 38(1), 1–13.
- Bauer, M., M. Bruveris, and P. W. Michor (2016). Why use Sobolev metrics on the space of curves? In *Riemannian Computing in Computer Vision*, pp. 233–255. Springer.
- Bauer, M., M. Eslitzbichler, and M. Grasmair (2015). Landmark-guided elastic shape analysis of human character motions. *arXiv preprint arXiv:1502.07666*.

- Bhattacharya, R. N. and V. Patrangenaru (2003). Large sample theory of intrinsic and extrinsic sample means on manifolds I. *The Annals of Statistics* 31(1), 1–29.
- Celledoni, E. and M. Eslitzbichler (2015). Shape analysis on lie groups with applications in computer animation. *arXiv preprint arXiv:1506.00783*.
- Chang, T. (1986). Spherical regression. *The Annals of Statistics* 14(3), 907–924.
- Chirikjian, G. S. and A. B. Kyatkin (2000). *Engineering applications of noncommutative harmonic analysis: with emphasis on rotation and motion groups*. CRC press.
- Davidson, J. (1994). *Stochastic limit theory: An introduction for econometricians*. OUP Oxford.
- Downs, T. D. (1972). Orientation statistics. *Biometrika* 59(3), 665–676.
- Dudek, E. and K. Holly (1994). Nonlinear orthogonal projection. In *Annales Polonici Mathematici*, Volume 59, pp. 1–31. Institute of Mathematics Polish Academy of Sciences.
- Duhamel, A., J. Bourriez, P. Devos, P. Krystkowiak, A. Destee, P. Derambure, and L. Defebvre (2004). Statistical tools for clinical gait analysis. *Gait & posture* 20(2), 204–212.
- Fletcher, T. (2011). Geodesic regression on riemannian manifolds. In *Proceedings of the Third International Workshop on Mathematical Foundations of Computational Anatomy-Geometrical and Statistical Methods for Modelling Biological Shape Variability*, pp. 75–86.
- Groen, B., M. Geurts, B. Nienhuis, and J. Duysens (2012). Sensitivity of the olga and vcm models to erroneous marker placement: effects on 3d-gait kinematics. *Gait & posture* 35(3), 517–521.
- Grood, E. S. and W. J. Suntay (1983). A joint coordinate system for the clinical description of three-dimensional motions: application to the knee. *Journal of biomechanical engineering* 105(2), 136–144.
- Helgason, S. (1962). *Differential Geometry and Symmetric Spaces*. New York: Academic Press.
- Huckemann, S. (2011). Inference on 3d Procrustes means: Tree bole growth, rank deficient diffusion tensors and perturbation models. *Scandinavian Journal of Statistics* 38(3), 424–446.
- Huckemann, S. (2012). On the meaning of mean shape: Manifold stability, locus and the two sample test. *Annals of the Institute of Statistical Mathematics* 64(6), 1227–1259.
- Kent, J. T. and K. V. Mardia (1997). Consistency of Procrustes estimators. *Journal of the Royal Statistical Society: Series B (Statistical Methodology)* 59(1), 281–290.
- Kurtek, S. A., A. Srivastava, and W. Wu (2011). Signal estimation under random time-warpings and nonlinear signal alignment. In J. Shawe-Taylor, R. Zemel, P. Bartlett, F. Pereira, and K. Weinberger (Eds.), *Advances in Neural Information Processing Systems 24*, pp. 675–683. Curran Associates, Inc.
- Leardini, A., L. Chiari, U. Della Croce, and A. Cappozzo (2005). Human movement analysis using stereophotogrammetry: part 3. soft tissue artifact assessment and compensation. *Gait & Posture* 21(2), 212–225.
- Lee, J. M. (2013). *Introduction to Smooth manifolds*. Springer Verlag, New York.
- Mebius, J. E. (2005). A matrix-based proof of the quaternion representation theorem for four-dimensional rotations. *arXiv preprint math/0501249*.
- Myers, S. B. and N. Steenrod (1939). The group of isometries of a Riemannian manifold. *Annals of Mathematics* 40(2), 400–416.

- Noehren, B., K. Manal, and I. Davis (2010). Improving between-day kinematic reliability using a marker placement device. *Journal of Orthopaedic Research* 28(11), 1405–1410.
- Õunpuu, S., M. Solomito, K. Bell, P. DeLuca, and K. Pierz (2015). Long-term outcomes after multilevel surgery including rectus femoris, hamstring and gastrocnemius procedures in children with cerebral palsy. *Gait & posture* 42(3), 365–372.
- Pierrynowski, M. R., P. A. Costigan, M. R. Maly, and P. T. Kim (2010). Patients with osteoarthritic knees have shorter orientation and tangent indicatrices during gait. *Clinical Biomechanics* 25(3), 237–241.
- Ramsay, J. (1982). When the data are functions. *Psychometrika* 47(4), 379–396.
- Rancourt, D., L.-P. Rivest, and J. Asselin (2000). Using orientation statistics to investigate variations in human kinematics. *Journal of the Royal Statistical Society: Series C (Applied Statistics)* 49(1), 81–94.
- Srivastava, A., E. Klassen, S. H. Joshi, and I. H. Jermyn (2011). Shape analysis of elastic curves in euclidean spaces. *Pattern Analysis and Machine Intelligence, IEEE Transactions on* 33(7), 1415–1428.
- Srivastava, A., W. Wu, S. Kurtek, E. Klassen, and J. S. Marron. Registration of functional data using fisher-rao metric. *arXiv preprint arXiv:1103.3817*.
- Stanfill, B., U. Genschel, and H. Hofmann (2013). Point estimation of the central orientation of random rotations. *Technometrics* 55(4), 524–535.
- Stuelpnagel, J. (1964). On the parametrization of the three-dimensional rotation group. *SIAM review* 6(4), 422–430.
- Su, J., S. Kurtek, E. Klassen, A. Srivastava, et al. (2014). Statistical analysis of trajectories on Riemannian manifolds: bird migration, hurricane tracking and video surveillance. *The Annals of Applied Statistics* 8(1), 530–552.
- Umeyama, S. (1991). Least-squares estimation of transformation parameters between two point patterns. *Pattern Analysis and Machine Intelligence, IEEE Transactions on* 13(4), 376–380.
- Wang, J.-L., J.-M. Chiou, and H.-G. Müller (2015). Review of functional data analysis. *Annu. Rev. Statist* 1, 41.
- Ziezold, H. (1977). Expected figures and a strong law of large numbers for random elements in quasi-metric spaces. *Transaction of the 7th Prague Conference on Information Theory, Statistical Decision Function and Random Processes A*, 591–602.